IMAGING RADAR CONTRIBUTIONS TO A MAJOR AIR-SEA-ICE INTERACTION STUDY IN THE GREENLAND SEA

Robert A. Shuchman*
Radar Science Laboratory
Environmental Research Institute of Michigan
Ann Arbor, Michigan

The Marginal Ice Zone (MIZ) is the region of the outermost extent of the polar ice field. The MIZ is the critical region in which polar air masses, ice and water masses interact with the temperate ocean and climate systems. The processes that take place there profoundly influence hemispheric climate and have a significant effect on petroleum/mineral exploration and production, naval operations, and commercial fishing. To gain an understanding of these processes sufficient to permit modeling and prediction, a research strategy was developed for summer and winter measurement programs (Wadhams et al., 1981), and a series of field experiments were planned and executed (Johannessen et al., 1983). One such experiment was conducted in the Fram Strait region of the Greenland Sea in the summer of 1983 and 1984. The purpose of the program in the Fram Strait was to study the mesoscale physical processes by which ice, ocean, and atmosphere interact in the MIZ in summer (Johannessen and Horn, 1984).

In this program synthetic aperture radar (SAR) was used as both a real-time reconnaissance tool as well as a scientific instrument. Due to extensive and persistant cloud cover over the MIZ, SAR data obtained from aircraft was the only means to provide weather independent data in real-time to the ice-strengthened ships conducting sea truth in the area. Figure 1 summarizes the coordination of the remote sensing activities during the 83 and 84 experiments. A field coordination center was maintained on the ice-strengthened ship R/V POLARSTERN that served as a center for all remote sensing ocean- and sea-ice-truth activities. A land coordination station, located at Tromso, Norway, interpreted aircraft and satellite data, and transmitted this information to the field center. The ship utilized the satellite information when available along with SAR provided data, voice communication from the various aircraft, directly received satellite data, and helicopter reconnaissance flights to direct the local remote sensing activities (helicopter, ship based, and surface).

The SAR data set collected on 5 July during the MIZEX program serves as an example of the remote sensing analyses possible. Mosaicked L-band (23-cm wavelength) imagery from that day is shown in Figure 2. The high reflectivity of the ice in the MIZ relative to that of open water is responsible for the excellent ice edge and floe definition seen in this imagery. Likewise, the structure in the three eddies visible in this image is well defined due to the high reflectivity of small, 50-500 m rough, broken floes entrained in the eddy currents. In the field, being able to locate eddies in real-time SAR output allowed research ships to be directed to active sites.

*Co-Chairman MIZEX Remote Sensing Group. This research was supported by ONR Contracts N00014-81-C-0295 and N00014083-C-0404. The ONR technical monitor is Mr. Charles Luther.

By collecting imagery over several days, it has been possible to monitor the evolution and motion of these eddy features, as well as the motion of floes throughout the MIZ ice field (Shuchman and Burns, 1985).

Manual interpretations done on the mosaics, such as the one for 5 July shown in Figure 2, are based on features observed in both the X-band (3-cm wavelength) and L-band data. These channels provide complementary information. The X-band gives better ice/water contrast and therefore good floe definition, whereas the L-band provided more detail on features within floes and, under some conditions, ocean wave features. In the case of the 5 July data, the melt water front and the ocean slicks that may be associated with internal waves are observed in the L-band but not in the X-band imagery.

The manual interpretation was carried out in three parts. The first was to identify unique features; eddies, large floes, polynyas, and internal waves. The second step was to segment ice-covered regions into areas with the same signatures; that is, the same perceived overall tone and texture. In general, each area or class appears to be associated with a different combination of ice concentration and floe size distribution. Step three was to then quantify the ice concentration and median floe size associated with each class. Using a machine-assisted manual analysis approach, representative subareas for each class were selected from the mosaic and located on the image strips. Floe boundaries for all floes within each subarea were then digitized using a DIGI-PAD 5 digitizer interfaced to a Z-100 micro-computer. Once in digital format, the data were manipulated to obtain area, perimeter, and diameter of each floe and total ice concentration of the subarea. The same approach has been applied to the multi-temporal SAR images to obtain maps of the ice field motion.

Values of ice concentration and floe size obtained in this way appear in the interpretation key (see Figure 2). The accuracy of this procedure was determined with data from 30 June 1984 where it was applied to both SAR imagery and coincident, near-simultaneous aerial photography also obtained by the CV-580. Discrepancy between SAR-derived and aerial photo concentration estimates was at most 5 percent for concentrations ranging from 30 percent to 80 percent. Correspondence between floe size was also evaluated and found to be within 5 percent on average.

In summary, by virtue of the SAR's imaging capabilities, such as all-weather imaging, relatively high resolution, and large dynamic range of backscatter from SAR ice and open ocean, information on the important MIZ parameters can be derived from the SAR data. Information on ice edge location and location of ice-edge eddies, for example, can be obtained directly from examination of the imagery as can detection of ocean fronts and internal waves. With machine-assisted manual image analysis, estimates of ice concentration, floe size distributions, and ice field motion can also be derived. Full digital analysis, however, is required to obtain gravity wave spectral information and backscatter statistics for ice type discrimination and automated ice concentration algorithms.

REFERENCES

Johannessen, O. M., W. D. Hibler III, P. Wadhams, W. J. Campbell, K. Hasselmann, I. Dyer, and M. Dunbar, MIZEX, A program for mesoscale air-ocean-ice interaction experiments in Arctic marginal ice zones, II. A science plan for a summer marginal ice zone experiment in the Fram Strait/ Greenland Sea (MIZEX Bulletin II), U.S. Army Cold Regions Research and Engineering Laboratory, CRREL Special Report 83-12, 1983.

Johannessen, O. M., and D. Horn (Ed.), MIZEX 84, Summer experiment PI preliminary reports (MIZEX Bulletin V), U.S. Army Cold Regions Research and Engineering Laboratory, CRREL Special Report 84-29, 1984.

Shuchman, R. A. and B. A. Burns, Remote sensing of the marginal ice zone during MIZEX 83 and 84, Proceedings of the Arctic Oceanography Conference and Workshop, NORDA, Hattiesburg, MS, June 1985, U.S. Dept. of the Navy, 178-189, 1985.

Wadhams, P., S. Martin, O. M. Johannessen, W. D. Hibler III, and W. J. Campbell (Ed.), MIZEX: A program for mesoscale air-ice-ocean interaction experiments in arctic marginal ice zones, I. Research strategy (MIZEX Bulletin II), U.S. Army Cold Regions Research and Engineering Laboratory, CRREL Special Report 81-19, June 1981.

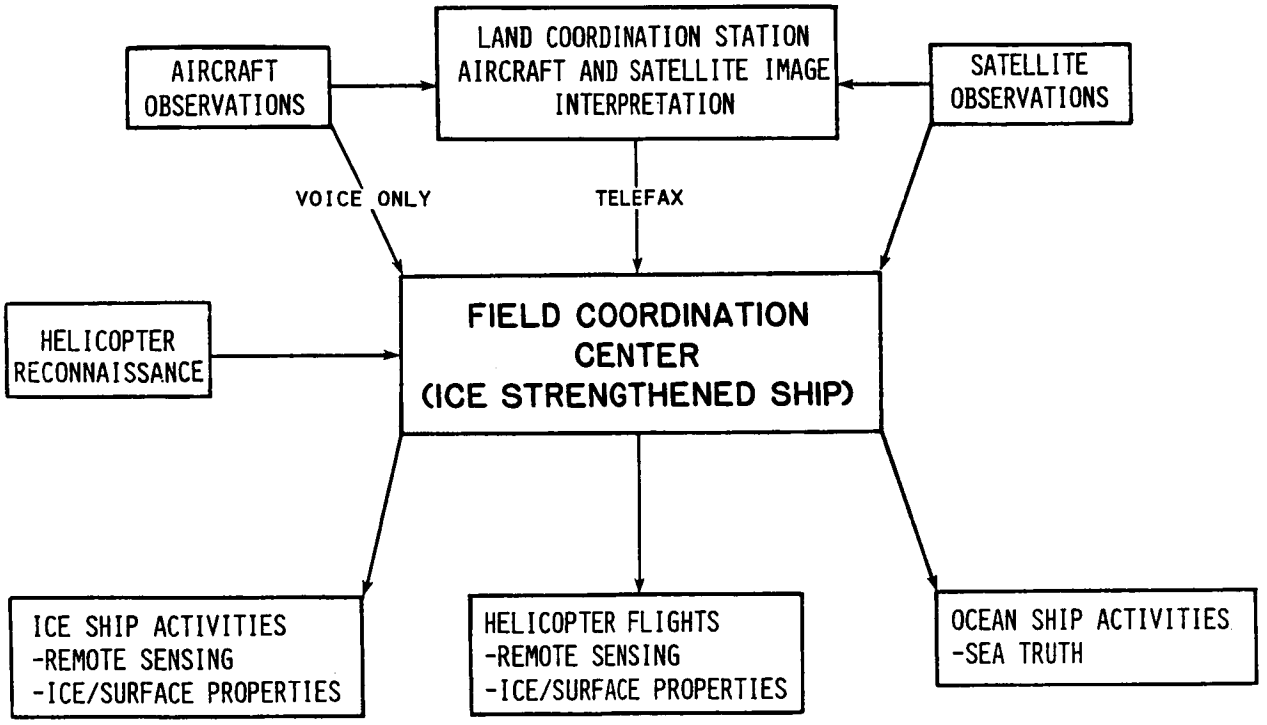

Figure 1. Approach utilized to coordinate the MIZEX 83 and 84 remote sensing activities

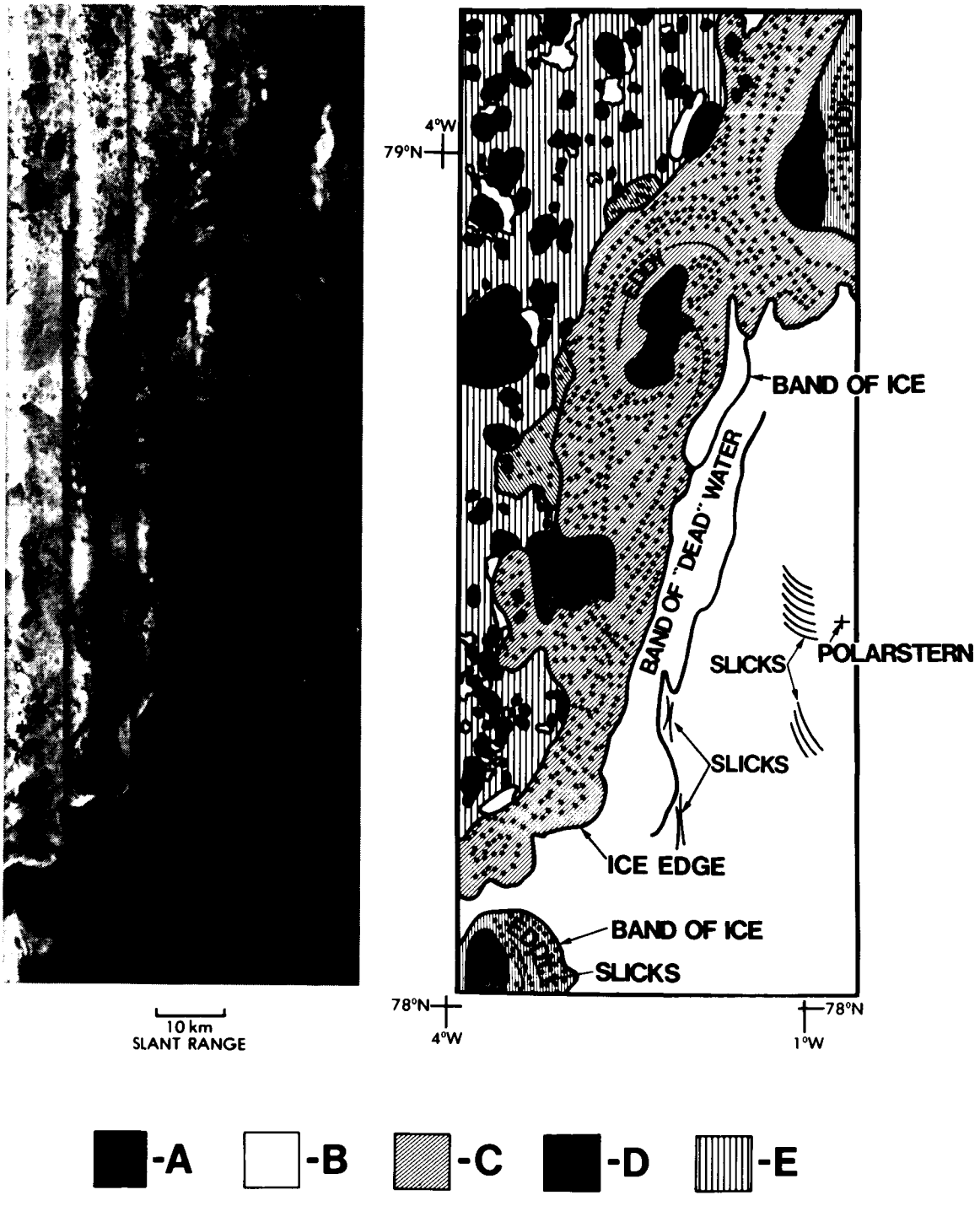

Figure 2. L-band (1.2 GHz) mosaic collected by the ERIM/CCRS X-C-L-band SAR system on 5 July 1984 (1400-1700 GMT). The large eddy is clearly visible on the 3m x 3m resolution data, as are large individual floes (labeled 'A' on the interpretation) and polynyas and ice-free ocean areas (labeled 'B'). The interpretation also indicates areas of varying ice concentration, the range of floe sizes, and the median size: 30%, 1-50m, 12m, for 'C'; 80%, 1-1500m, 150m for 'D'; and 80%, 10m-6km, 1km for 'E', respectively.